

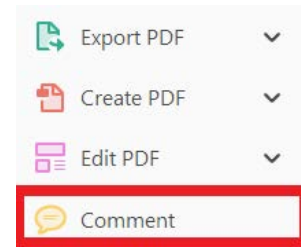
USING e-ANNOTATION TOOLS FOR ELECTRONIC PROOF CORRECTION

Required software to e-annotate PDFs: Adobe Acrobat Professional or Adobe Reader (version 11 or above). (Note that this document uses screenshots from Adobe Reader DC.)

The latest version of Acrobat Reader can be downloaded for free at: <http://get.adobe.com/reader/>

Once you have Acrobat Reader open on your computer, click on the Comment tab (right-hand panel or under the Tools menu).

This will open up a ribbon panel at the top of the document. Using a tool will place a comment in the right-hand panel. The tools you will use for annotating your proof are shown below:

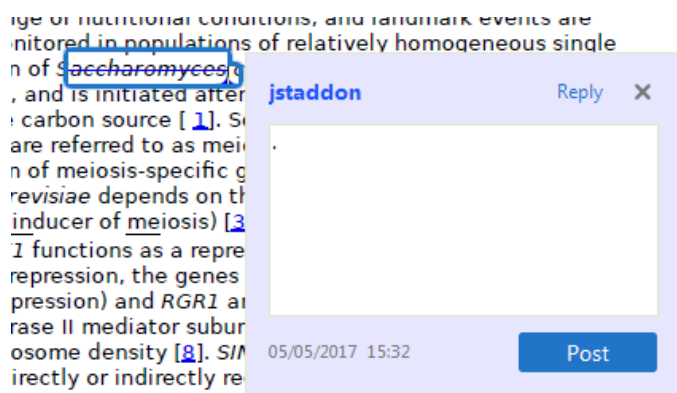


1. **Replace (Ins) Tool** – for replacing text.

 Strikes a line through text and opens up a text box where replacement text can be entered.

How to use it:

- Highlight a word or sentence.
- Click on .
- Type the replacement text into the blue box that appears.



2. **Strikethrough (Del) Tool** – for deleting text.

 Strikes a red line through text that is to be deleted.

How to use it:

- Highlight a word or sentence.
- Click on .
- The text will be struck out in red.

experimental data if available. For ORFs to be had to meet all of the following criteria:

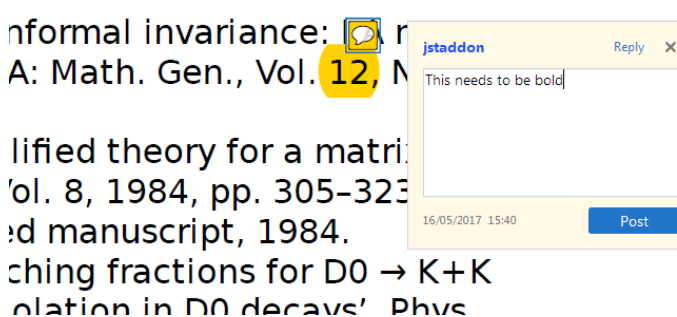
1. Small size (35-250 amino acids).
2. Absence of similarity to known proteins.
3. Absence of functional data which could not be the real overlapping gene.
4. Greater than 25% overlap at the N-terminus terminus with another coding feature; over both ends; or ORF containing a tRNA.

3. **Commenting Tool** – for highlighting a section to be changed to bold or italic or for general comments.

  Use these 2 tools to highlight the text where a comment is then made.

How to use it:

- Click on .
- Click and drag over the text you need to highlight for the comment you will add.
- Click on .
- Click close to the text you just highlighted.
- Type any instructions regarding the text to be altered into the box that appears.

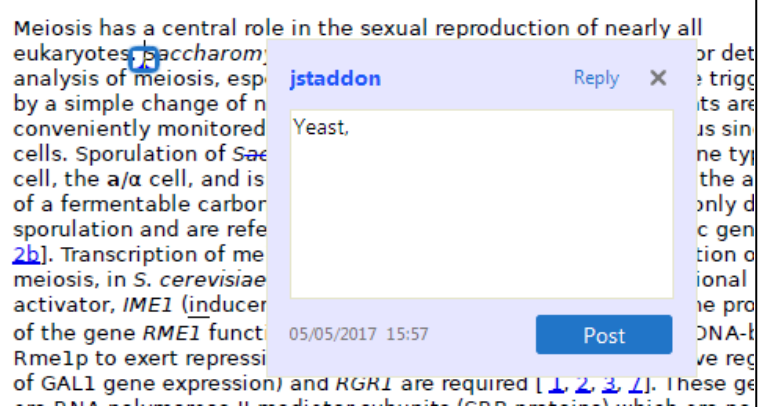


4. **Insert Tool** – for inserting missing text at specific points in the text.

 Marks an insertion point in the text and opens up a text box where comments can be entered.

How to use it:

- Click on .
- Click at the point in the proof where the comment should be inserted.
- Type the comment into the box that appears.



5. Attach File Tool – for inserting large amounts of text or replacement figures.

 Inserts an icon linking to the attached file in the appropriate place in the text.

How to use it:

- Click on .
- Click on the proof to where you'd like the attached file to be linked.
- Select the file to be attached from your computer or network.
- Select the colour and type of icon that will appear in the proof. Click OK.

The attachment appears in the right-hand panel.

chondrial preparator
ative damage injury
re extent of membra
i, malondialdehyde (TBARS) formation.
used by high perform

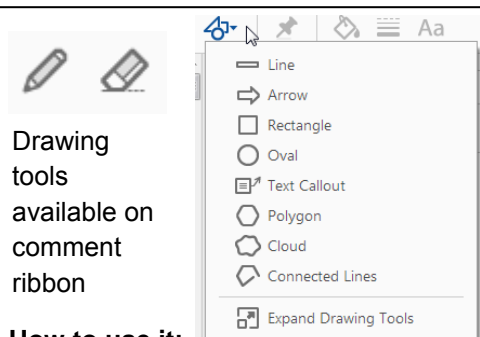
6. Add stamp Tool – for approving a proof if no corrections are required.

 Inserts a selected stamp onto an appropriate place in the proof.

How to use it:

- Click on .
- Select the stamp you want to use. (The **Approved** stamp is usually available directly in the menu that appears. Others are shown under *Dynamic*, *Sign Here*, *Standard Business*).
- Fill in any details and then click on the proof where you'd like the stamp to appear. (Where a proof is to be approved as it is, this would normally be on the first page).

of the business cycle, starting with the
on perfect competition, constant ret
production. In this environment goods
extra costs should be set to market
he market is determined by the model. The New-Key
otaki (1987), has introduced produc
general equilibrium models with nomin
and downward sloping. Most of this literat

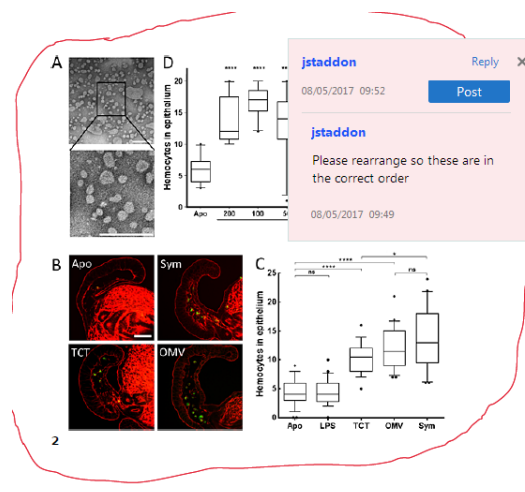


How to use it:

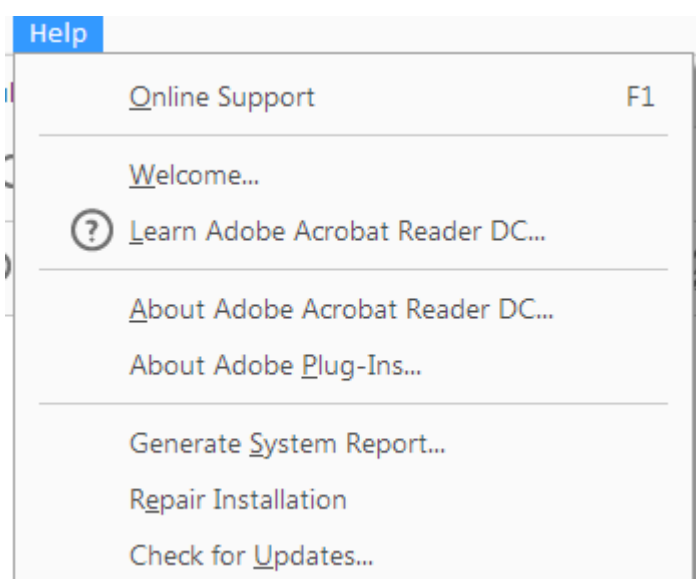
- Click on one of the shapes in the **Drawing Markups** section.
- Click on the proof at the relevant point and draw the selected shape with the cursor.
- To add a comment to the drawn shape, right-click on shape and select *Open Pop-up Note*.
- Type any text in the red box that appears.

7. Drawing Markups Tools – for drawing shapes, lines, and freeform annotations on proofs and commenting on these marks.

Allows shapes, lines, and freeform annotations to be drawn on proofs and for comments to be made on these marks.



For further information on how to annotate proofs, click on the **Help** menu to reveal a list of further options:



Author Query Form

Journal: Polymers for Advanced Technologies

Article: pat_4511

Dear Author,

During the copyediting of your paper, the following queries arose. Please respond to these by annotating your proofs with the necessary changes/additions.

- If you intend to annotate your proof electronically, please refer to the E-annotation guidelines.
- If you intend to annotate your proof by means of hard-copy mark-up, please use the standard proofing marks. If manually writing corrections on your proof and returning it by fax, do not write too close to the edge of the paper. Please remember that illegible mark-ups may delay publication.

Whether you opt for hard-copy or electronic annotation of your proofs, we recommend that you provide additional clarification of answers to queries by entering your answers on the query sheet, in addition to the text mark-up.

Query No.	Query	Remark
Q1	AUTHOR: You have provided all figures 1,2,3,4,5 in colour. Because of the high cost of colour printing we can only print the figures in colour if authors cover the expense. However, the figures will be published online in colour free of cost. Please confirm if you would like the figure(s) to be printed in colour.	B & W in print is OK.
Q2	AUTHOR: Please confirm that forenames/given names (blue) and surnames/family names (vermilion) have been identified correctly.	OK
Q3	AUTHOR: Please verify that the linked ORCID identifier is correct.	OK

Please confirm that the funding sponsor list below was correctly extracted from your article: that it includes all funders and that the text has been matched to the correct FundRef Registry organization names. If a name was not found in the FundRef registry, it may not be the canonical name form, it may be a program name rather than an organization name, or it may be an organization not yet included in FundRef Registry. If you know of another name form or a parent organization name for a “not found” item on this list below, please share that information.

FundRef Name	FundRef Organization Name
Ministry of Education, Culture, Sports, Science and Technology	Ministry of Education, Culture, Sports, Science and Technology

Solid polymer electrolytes based on polystyrene-polyether block copolymers having branched ether structure

Hisashi Kokubo  | Eiji Nakazawa | Masayoshi Watanabe 

Department of Chemistry and Biotechnology,
Yokohama National University, Yokohama,
Japan

Correspondence

Masayoshi Watanabe, Department of
Chemistry and Biotechnology, Yokohama
National University, 79-5 Tokiwadai,
Hodogaya-ku, Yokohama 240-8501, Japan.
Email: mwatanab@ynu.ac.jp

Funding information

Ministry of Education, Culture, Sports, Science
and Technology, Grant/Award Number:
15H05758

To obtain solid polymer electrolytes (SPEs) having high ionic conductivity together with mechanical integrity, we have synthesized polystyrene (PSt)-polyether (PE) diblock copolymers via one-pot anionic polymerization. The PSt block is expected to aggregate to act as hard fillers in the SPE to enhance the mechanical property. The PE block consists of random copolymer (P-(EO-*r*-MEEGE)) of ethylene oxide (EO) and 2-(2-methoxyethoxy) ethyl glycidyl ether (MEEGE) in different molar ratios ([EO]/[MEEGE] = 100/0, 86/14, 75/25, 68/32, and 41/59). The introduction of the MEEGE moiety in PEO reduced the crystallinity of PEO, and the fast motion of the MEEGE side chain caused plasticization of the PE block, thereby contributing to the fast ion transport. SPEs were fabricated by mixing the obtained diblock copolymer (PSE_{*x*}) and lithium bis(trifluoromethanesulfonyl) amide (LiTFSA) with [Li]/[O] = 0.05. Ionic conductivity of the obtained SPEs was dependent on the molar ratio of EO in the PE block (*x*) as well as the weight fraction of PE block (*f*_{PE}) in the block copolymer. PSE_{0.86} (*f*_{PE} = 0.65) exhibited high ionic conductivity ($3.3 \times 10^{-5} \text{ S cm}^{-1}$ at 30°C; $1.1 \times 10^{-4} \text{ S cm}^{-1}$ at 60°C) comparable with that of P-(EO-*r*-MEEGE) (PE_{0.85}; *f*_{PE} = 1.00) ($9.8 \times 10^{-5} \text{ S cm}^{-1}$ at 30°C; $4.0 \times 10^{-4} \text{ S cm}^{-1}$ at 60°C).

KEYWORDS

block copolymer, one-pot living anionic polymerization, solid polymer electrolytes

1 | INTRODUCTION

Since the first proposal on solid polymer electrolytes (SPEs), consisting of poly(ethylene oxide) (PEO) and lithium salt,¹ for application in lithium batteries, a number of researches on SPEs have been reported.²⁻³⁵ Typical SPEs consist of polyethers (PEs) and lithium salts, where the lithium cations are coordinated by the ether oxygen atoms, and can move in synchronization with the segmental motion of the PE chain. To enhance the ionic conductivity of PEO-based SPEs, suppression of crystallization and decrease in glass transition temperature (*T*_g) of the PEO are generally required. While the ionic conductivity of the SPEs increases with an increase in salt concentration because of an increase in the number of the mobile carrier, a decrease in the conductivity becomes apparent at higher salt concentrations, resulting from a decrease in the carrier mobility owing to an increase in *T*_gs, which is caused by pseudo cross-linking between the lithium cation and the ether oxygen atoms. In order to increase the

ionic conductivity of SPEs, we have proposed introduction of an oligo-ether side chain on the PEO main chain.¹⁰⁻¹⁵ Owing to the faster molecular motion and its smaller temperature dependency of the side chain than those of the main chain, high ionic conductivity can be attained. Specifically, a random copolymer, poly(ethylene oxide-*r*-2-(2-methoxyethoxy) ethyl glycidyl ether) (P-(EO-*r*-MEEGE)), polymerized from ethylene oxide (EO) and 2-(2-methoxyethoxy) ethyl glycidyl ether (MEEGE) was designed, and P-(EO-*r*-MEEGE) ([EO]/[MEEGE] = 73/27 mol/mol; [Li]/[O] = 0.06) electrolyte showed high ionic conductivity ($3.3 \times 10^{-4} \text{ S cm}^{-1}$ at 30°C; $1.4 \times 10^{-3} \text{ S cm}^{-1}$ at 60°C).¹³ A polymer electrolyte of a chemically cross-linked P-(EO-*r*-MEEGE) network having mechanical integrity also maintained high conductivity ($4.0 \times 10^{-4} \text{ S cm}^{-1}$ at 60°C; [Li]/[O] = 0.04; [EO]/[MEEGE] = 85/15).¹⁴ However, since the chemically cross-linked polymer networks cannot be further processed neither thermally nor via solution, SPEs using block copolymers have been proposed.¹⁸⁻³⁶ The block copolymers consisting of a soft segment such

as PE and a hard segment with high T_g such as polystyrene (PSt) show a microphase separation in the solid state.^{18-35,37} An ion conduction path is formed by the PE soft segments, and the aggregation of the hard segment acts as hard fillers and/or physical cross-linking points. Thus, the polymer electrolytes can be processed from solutions or from melts by heating above T_g of the hard segments. Moreover, use of PSt and PE is also beneficial in terms of polymer synthesis. These polymers are easily obtained with a molecular weight determined and with a relatively narrow polydispersity index via living polymerization method. Therefore, molecular weight dependence is easy to investigate, and distinct microphase separation structure is expected.

Herein, we propose SPEs utilizing the diblock copolymers consisting of PSt and P-(EO-*r*-MEEGE), having both thermoplasticity and high ionic conductivity. The diblock copolymer is represented as PSE_x, where the subscript "x" indicates molar ratio of the EO unit in the synthesized PE segment ($[\text{EO}]/([\text{EO}] + [\text{MEEGE}])$). The PSE_xs with several x values were synthesized under the following regulations: (1) total molecular weight ($M_{n,\text{total}}$) is ca. 20 000 and (2) weight fraction of PE block segment (f_{PE}) is ca. 0.6. In addition to the PSE_xs, we also prepared PSE having a large f_{PE} (named as L-PSE_x) in order to investigate the effect of PE fraction in the block copolymer on the ionic conductivity and rheological property.

2 | EXPERIMENTAL SECTION

2.1 | Materials

Dehydrated tetrahydrofuran (THF) (Kanto Chemical), dehydrated dimethyl sulfoxide (DMSO) (Kanto Chemical), 1 M *sec*-butyl lithium (*sec*-BuLi) in hexane solution (Kanto Chemical), 2,2-diethyl-1,3-propanediol (DEPD) (TCI), 1 M phosphazene base (*t*-BuP₄) in hexane (Sigma-Aldrich), and lithium bis(trifluoromethanesulfonyl)amide (LiTFSA) (Morita Chemical) were used without further purification. Ethylene oxide (EO) was purchased from NOF Corporation and purified by distillation after drying with calcium hydride. MEEGE was synthesized according to the reported procedure.^{12,14} Styrene (Wako Chemical) was distilled under vacuum with calcium hydride prior to use. THF solution of potassium naphthalene was prepared according to the method reported in literature, and its concentration was determined by titration using aqueous hydrochloric acid.^{38,39}

2.2 | Measurements

¹H NMR spectra were recorded on a JEOL AL400 spectrometer in CDCl₃. Gel permeation chromatography (GPC) measurements (eluent: THF; detector: refractive index (RI)) were performed on a SHIMADZU GPC system equipped with two TSKGEL Multipore HXL-M (TOSOH) columns and analyzed by using PSt standards. Thermogravimetric (TG) analysis and differential scanning calorimetry (DSC) analysis were conducted by a TG/DTA6200 (Seiko Instruments) and a DSC220C (Seiko Instruments), respectively. The TGA samples were put in an Al-pan and heated from 30°C to 550°C at a rate of 10°C minute⁻¹ under nitrogen atmosphere. Ten milligrams

of DSC samples encapsulated into an Al-pan were firstly heated at 120°C and then cooled to -150°C. The second scan was recorded from -150°C to 120°C at a heating rate of 10°C minute⁻¹. The ionic conductivities of the polymer electrolytes were measured by an LF Impedance Analyzer 4192A (Hewlett Packard) over a frequency range of 5 Hz to 13 MHz. The samples were sandwiched by two stainless steel disk electrodes separated by a polytetrafluoroethylene (PTFE) spacer with an inner diameter of 13 mm and thickness of 1 mm. The cell constant was evaluated by 0.01 mol L⁻¹ potassium chloride aqueous solution at 25°C. The temperature dependence measurements were carried out during cooling from 100°C to 0°C after allowing the sample at each temperature for 1 hour. The rheological measurements were conducted by a Physica MCR301 (Anton Paar) equipped with a Peltier-type temperature control system. A parallel plate of 25-mm diameter was used as a measuring jig.

2.3 | Synthesis of block copolymers, PSt-*b*-P-(EO-*r*-MEEGE) (PSE_xs)

In case of a feed molar ratio of $[\text{EO}]/[\text{MEEGE}] = 9/1$ (PSE_{0.86}), 1.0 mL of 1 M *sec*-BuLi/hexane solution was dissolved in 50 mL of dehydrated THF under nitrogen at -78°C. Then, 6.6 mL of styrene (58 mmol) was added promptly into the solution and stirred for 1 hour followed by continuous addition of 6.7 mL of EO (135 mmol) and 2.5 mL of MEEGE (16 mmol) and stirred for 1 hour at -78°C. After the temperature was gradually increased to 0°C for 3 hours, 1.0 mL of *t*-BuP₄ (1.0 mmol) was added to the solution and stirred for 4 days at room temperature. The polymerization reaction was terminated by addition of a 1 M hydrochloric acid. The precipitated salt was removed by suction filtration, and the reprecipitation was carried out three times by using THF as a good solvent and hexane as a poor solvent. Light yellow powder was obtained after vacuum drying. The other PSE_xs were prepared in the similar manner as PSE_{0.86}. For L-PSE_{0.73} with high total molecular weight, 0.5 mL of 1 M *sec*-BuLi/hexane solution was dissolved in 40 mL of dehydrated THF under nitrogen at -78°C. Then, 5.5 mL of styrene (48 mmol) was added promptly into the solution and stirred for 1 hour followed by continuous addition of 3.5 mL of EO (70 mmol) and 5.0 mL of MEEGE (31 mmol) that were continuously added into the reaction solution and stirred for 1 hour at -78°C. After the temperature was gradually increased to 0°C, 0.75 mL of *t*-BuP₄ (0.75 mmol) was added into the reaction solution. After ascertaining the consumption of MEEGE through gas chromatography, 3.5 mL of EO (70 mmol) and 5.0 mL of MEEGE (31 mmol) were added again and the solution was stirred for 4 days at room temperature. The polymerization reaction was stopped by adding 1 M hydrochloric acid. The precipitated salt was removed by suction filtration, and the reprecipitation was carried out three times by using hexane. The obtained polymer was dissolved in THF, and the solution was passed through a basic alumina column, followed by a reprecipitation procedure. Light yellow powder was obtained after vacuum drying. ¹H NMR (CDCl₃, 400 MHz) δ : 6.58-7.08 (m, Ar-*H* of PSt), 3.45-3.75 (m, CH₂ and CH of PE), 3.38 (s, CH₃ of MEEGE), 1.28-1.84 (m, CH₂ and CH of PSt).

2.4 | Synthesis of P-(EO-*r*-MEEGE) (PE_{0.85})

First, 105 mg of DEPД (0.75 mmol) was dissolved in 30 mL of dehydrated THF under nitrogen. Then, 4.71 mL of 0.32 M potassium naphthalene (1.5 mmol) was added into the reaction solution and stirred for 1 hour at 0°C, followed by the addition of 20 mL of dehydrated DMSO and again stirred for 1 hour at 0°C. After stirring for 1 hour, 10.5 mL of EO (211 mmol) and 15 mL of MEEGE (94 mmol) were continuously added into the solution and stirred for 1 hour at 0°C, and then, the temperature of the reaction solution was gradually increased to room temperature, and stirred for 60 hours. The reaction was then stopped by adding 1 M hydrochloric acid. The precipitated salt was removed by suction filtration, and the reprecipitation was conducted three times by using a cold diethyl ether cooled in dry ice-methanol bath. The obtained polymer was dissolved in dichloromethane and passed through the basic alumina column. The reprecipitation was conducted again, and the light yellow solid was obtained after vacuum drying. Molecular weight and molar ratio of EO segment (*x*) of the resultant polymer evaluated by ¹H NMR was 32 000 and 0.85, respectively. ¹H NMR (CDCl₃, 400 MHz) δ: 3.45-3.75 (m, CH₂ and CH of PE main chain), 3.38 (s, CH₃ of MEEGE), 1.25 (q, CH₂ of DEPД), 0.78 (t, CH₃ of DEPД).

2.5 | Preparation of Li-doped PSE_{*x*} electrolyte membranes

Polymer electrolyte membranes consisting of PSE_{*x*} and LiTFSА were prepared by solution cast method. LiTFSА was dissolved in a THF solution of 10 wt% PSE_{*x*} at [Li]/[O] = 0.05, and stirred for 6 hours. The resultant solution was cast on a polyethylene terephthalate (PET) sheet surrounded by a silicone wall with a height of 0.5 mm. The sheets were placed under ambient atmosphere overnight, and then dried under vacuum at 60°C for 12 hours. Transparent and self-standing polymer electrolyte films were peeled from the PET sheet.

3 | RESULTS AND DISCUSSION

3.1 | Synthesis of PSE_{*x*}s and fabrication of electrolyte membrane

Block copolymer PSE_{*x*}s consisting of PSt and P-(EO-*r*-MEEGE) were synthesized via one-pot anionic polymerization as shown in Scheme 1. The PSt segment was initially polymerized from *sec*-butyl carbanion,

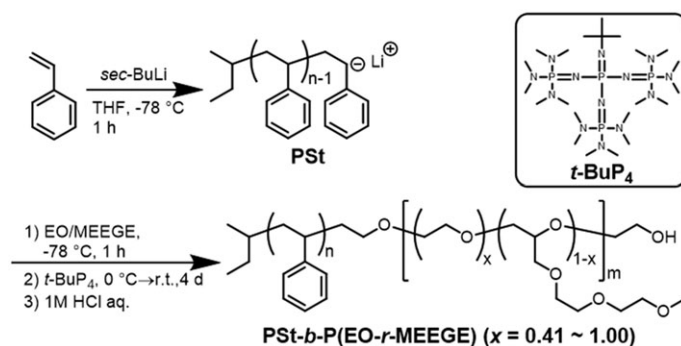
and then, EO and MEEGE were added into the reaction solution. For the polymerization of EO and MEEGE, the polymer ends were —CH₂CH₂O[−]Li⁺ (or —CH₂CHRO[−]Li⁺, where R is the side chain of MEEGE) resulting from the reaction between the carbanion at the “living” reaction end of PSt and one EO (or MEEGE) molecule.⁴⁰⁻⁴³ However, the polymer ends are inactive for the ring-opening anionic polymerization of EO and MEEGE owing to the formation of a strong ion pair between the alcoholate anion and lithium cation. *t*-BuP₄, which has strong Lewis basicity and coordinates to the lithium cation, was added into the reaction mixture for the progress of the polymerization reaction between EO and MEEGE, wherein the polymer ends became active for ring-opening anionic polymerization.⁴¹⁻⁴³

We have synthesized five PSE_{*x*}s with different molar ratios of EO and MEEGE, which were estimated from the ratio of the integration value of the methyl proton (δ 3.38) at the end of MEEGE side chain and another methylene and methine protons (δ 3.45-3.75) from their ¹H NMR spectra (Figure S1). The calculated molar ratios of the EO in the PE block segment were 1.00 (PSE_{1.00}), 0.86 (PSE_{0.86}), 0.75 (PSE_{0.75}), 0.68 (PSE_{0.68}), and 0.41 (PSE_{0.41}) with weight fraction of PE segment in the resultant PSE_{*x*}s (*f*_{PE}) of 0.52 to 0.65. All PSE_{*x*}s, except for PSE_{0.41}, showed total molecular weight (*M*_{n,total}) of ca. 20 000 as expected and narrow polydispersity index (*M*_w/*M*_{n,total}) (Table 1). Monomodal GPC curves of the PSE_{*x*}s and PSt macromonomer were observed (Figure S2), indicating that PE block was successfully polymerized from the carbanion PSt ends. Since [EO]/[MEEGE] in feed and that in the copolymer are nearly consistent, the reactivity of EO and MEEGE as a monomer of anionic polymerization is the same. We have also synthesized L-PSE_{0.73} with high *f*_{PE} (= 0.75) in order to probe the effect of *f*_{PE} on the ionic conductivity and rheological property.

The obtained PSE_{*x*} electrolyte membrane had poor film formability, and self-standing thin film could not be prepared, because the PSE_{*x*}s are cross-linked at only one polymer end. However, we could obtain self-standing membrane when the thickness was ca. 500 μm, as showing in Figure S3.

3.2 | Thermal properties of PSE_{*x*}

Thermal decomposition temperatures of all the synthesized PSE_{*x*}s were higher than 340°C, regardless of the ratio of [EO]/[MEEGE] (Figure S4). Table 2 summarizes the melting points (*T*_ms) and *T*_gs of the nondoped and Li-doped PSE_{*x*}s. Figure 1A shows the DSC curves of the nondoped PSE_{*x*}s. The *T*_m peak of PSE_{1.00} associated with



SCHEME 1 Synthetic route of PSt-P-(EO-*r*-MEEGE) block copolymers (PSE_{*x*}s)

TABLE 1 Molecular weight characteristics of the synthesized PSE_x block copolymers

PSE _x	M _{n,PSt} ^a	M _w /M _{n,PSt} ^a	[EO]/[MEEGE] (Molar Ratio)		M _{n,PE} ^b	M _{n,total}	M _w /M _{n,total} ^b	f _{PE} ^c
			In Feed	In Copolymer ^b				
PSE _{1.00}	8500	1.21	1.0/0.0	1.00/0.00	11 300	19 800	1.04	0.57
PSE _{0.86}	7400	1.29	0.9/0.1	0.86/0.14	13 600	21 000	1.28	0.65
PSE _{0.75}	9100	1.20	0.8/0.2	0.75/0.25	10 200	19 300	1.35	0.53
PSE _{0.68}	8400	1.21	0.7/0.3	0.68/0.32	11 300	19 700	1.37	0.57
PSE _{0.41}	6500	1.38	0.5/0.5	0.41/0.59	7100	13 600	1.26	0.52
L-PSE _{0.73}	9400	1.21	0.7/0.3	0.73/0.27	28 200	37 600	1.17	0.75

^aDetermined by GPC analysis.

^bDetermined by ¹H NMR analysis.

^cM_{n,PE}/M_{n,total}.

TABLE 2 Thermal properties of the PSE_xs for nondoped ([Li]/[O] = 0) and Li-doped ([Li]/[O] = 0.05) PSE_xs

Diblock Copolymer	[Li]/[O] = 0			[Li]/[O] = 0.05		
	T _m ^c , °C	T _{g,PE} ^a , °C	T _{g,PSt} ^c , °C	T _m ^c , °C	T _{g,PE} ^a , °C	T _{g,PSt} ^c , °C
PSE _{1.00}	43.9	-53.8	84	17.3	-44.7	84
PSE _{0.86}	-4.9	-64.8	72	-	-52.5	71
PSE _{0.75}	-	-65.7	76	-	-52.8	74
PSE _{0.68}	-	-67.5	76	-	-51.5	71
PSE _{0.41}	-	-65.1	79	-	-49.1	75
L-PSE _{0.73}	-17.8	-67.1	77	-	-52.0	n.d.

Abbreviation: n.d., not determined.

^aT_g derived from polyether block.

^bT_g derived from PSt block.

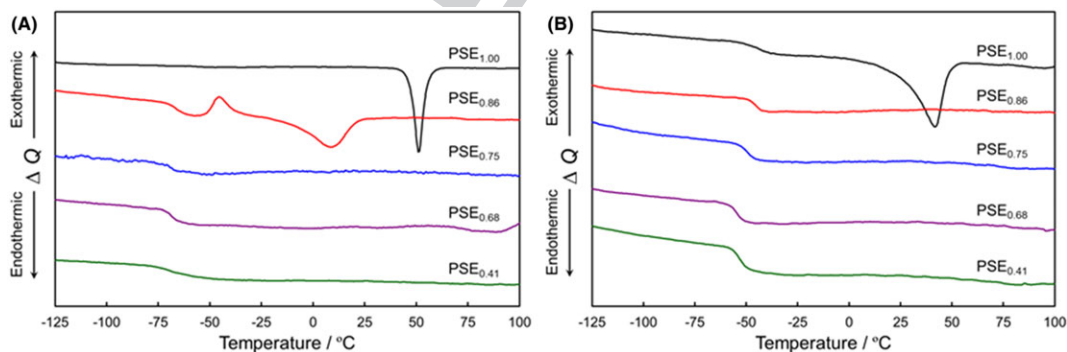


FIGURE 1 DSC curves of (A) nondoped PSE_xs ([Li]/[O] = 0) and (B) LiTFSA-doped PSE_xs ([Li]/[O] = 0.05) at a heating rate of 10°C minute⁻¹ [Colour figure can be viewed at wileyonlinelibrary.com]

crystallization of PEO was observed at 43.9°C, and that of PSE_{0.86} shifted to lower temperature at -4.9°C. T_ms of PSE_xs for x = 0.75, 0.68, and 0.41 were not observed, indicating that the PE segment became amorphous owing to the randomly introduced MEEGE structure into PEO. Two T_gs derived from PE and PSt were observed, indicating that microphase separation structure was formed.

As shown in Figure 1B, T_g of all the Li-doped PSE_xs increased by about 10°C in contrast to the corresponding nondoped PSE_xs, which could be attributed to a decrease in the segmental motion of PE chain caused by the inter and intra cross-linking due to the complex formation between the lithium ions and oxygen atoms in the PE chain. T_gs of

PSt were observed at a temperature equal to or slightly lower than that of undoped system. However, the distinct T_g of L-PSE_{0.73} could not be determined due to too small changes in the heat capacity around T_g, resulting from large f_{PE}.

3.3 | Effect of f_{PE} on the rheological properties

Figure 2 shows temperature dependence of storage modulus (G') and loss modulus (G'') for PSE_{0.68} (f_{PE} = 0.57) and L-PSE_{0.73} (f_{PE} = 0.75). PSE_{0.68} showed several times higher G' value than L-PSE_{0.73} at room

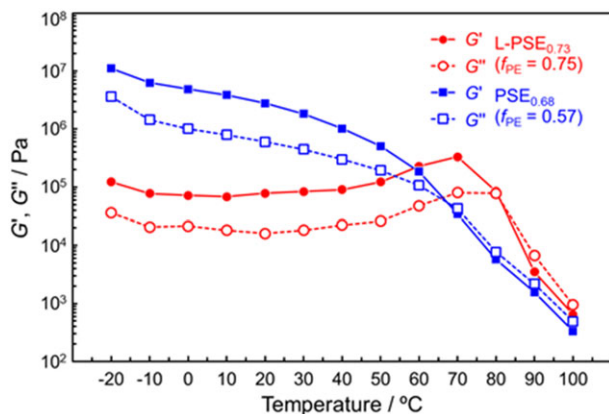


FIGURE 2 Temperature dependence of storage modulus (G') and loss modulus (G'') for $PSE_{0.68}$ and $L-PSE_{0.73}$ with $[Li]/[O] = 0.05$ at $\omega = 1 \text{ rad second}^{-1}$ [Colour figure can be viewed at wileyonlinelibrary.com]

temperature as $PSE_{0.68}$ has larger weight fraction of the PSt block segment. As the temperature increased, the G' and G'' of $PSE_{0.68}$ exhibited a crossover at 70°C , where coincided with T_g of PSt and $PSE_{0.68}$ started to flow, whereas the crossover temperature of $L-PSE_{0.73}$ appeared at a higher temperature of 80°C . The difference in the softening temperature may result from the difference in the segmental motion of the PE block. The T_g of PSt having molecular weight of 9000 lies at ca. 90°C .⁴⁴ The mobility of the PE in $PSE_{0.68}$ would be high owing to the less effect of the polymer entanglement, and the aggregation of the PSt might be suppressed. As a result, the softening temperature decreases below T_g of PSt homopolymer. On the contrary, the mobility of the PE chain in $L-PSE_{0.73}$ is limited due to the entanglement of the long PE chain behaving as a pseudo cross-linking point, resulting in the inhibition of decrease in the plasticizing temperature. Consequently, the polymer entanglement may affect the rheological property of the block copolymer. In addition, G' of $L-PSE_{0.73}$ exhibited a rubbery plateau in the temperature range between -20°C and 50°C , possibly resulting from the effect of polymer entanglement.

3.4 | Ionic conductivity

The Arrhenius plots of the ionic conductivity for the Li-doped PSE_x s ($[Li]/[O] = 0.05$) are shown in Figure 3. The plots for P-(EO-*r*-MEEGE) ($T_g = -52.3^\circ\text{C}$) having x value of 0.85 without PSt block ($PE_{0.85}$; $[Li]/[O] = 0.05$) are also shown for the comparison. A large decrease in the conductivity of $PSE_{1.00}$ observed at temperatures below 50°C corresponded to the crystallization process of PEO chain, since the measurement was conducted with cooling. Actually, the T_m peak of $PSE_{1.00}$ was observed around 50°C in the DSC curve conducted heating (Figure 1B). Other PSE_x s did not exhibit a sudden change in the conductivity because of amorphous nature of the PE block segments (Figure 1B).

$PSE_{0.86}$ showed the highest conductivity in the block copolymer electrolytes, which is about 60% of that of $PE_{0.85}$ (without PSt segment) in the measuring temperature range. It has been reported

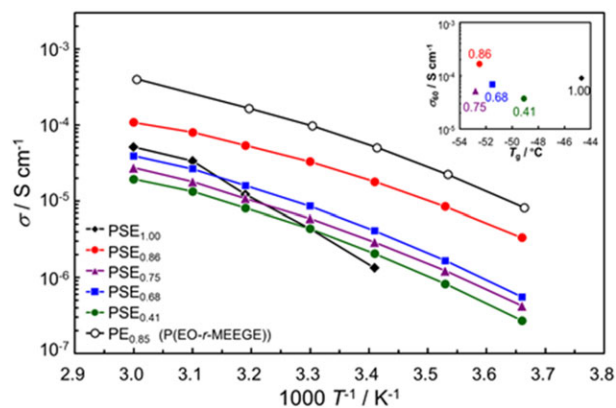


FIGURE 3 Temperature dependence of ionic conductivity for PSE_x s and $PE_{0.85}$ (P-(EO-*r*-MEEGE); $x = 0.85$). $[Li]/[O]$ is 0.05 for all the polymer electrolytes. Inset: Relationship between T_g and ionic conductivity at 60°C of PSE_x s with $[Li]/[O] = 0.05$. The symbols are the same as those in the Arrhenius plots [Colour figure can be viewed at wileyonlinelibrary.com]

that P-(EO-*r*-MEEGE) doped with LiTfSA exhibits a conductivity maximum at $x = 0.8$ to 0.7 ,¹³ owing to the fast molecular motion of the MEEGE side chains. However, as shown in the inset of Figure 3, the ionic conductivity at 60°C did not simply correlate with the T_g values. $PSE_{0.86}$ has higher weight fraction of the PE block segment ($f_{PE} = 0.65$) than another PSE_x s ($f_{PE} = 0.52$ – 0.57), which contributes to an increase in the fraction of the ion conduction path, since the block copolymers, whose segments are incompatible with each other, form phase-separated structure depending on the fraction of each block.^{18–20,22–35,37}

Figure S5 shows Arrhenius plots of ionic conductivity for $PE_{0.85}$ (without PSt segment), $L-PSE_{0.73}$, and $PSE_{0.68}$ ($[Li]/[O] = 0.05$) with different f_{PE} of 1.0, 0.75, and 0.57, respectively, wherein it showed that the higher the f_{PE} , the higher is the conductivity. This result supports that the formation of the continuous phase relies on f_{PE} values. Figure 4 displays the relationship between the ionic conductivity and f_{PE} values at 30°C and 60°C . It is clearly evident that the conductivity gradually decreases with decreasing the weight fraction of PE

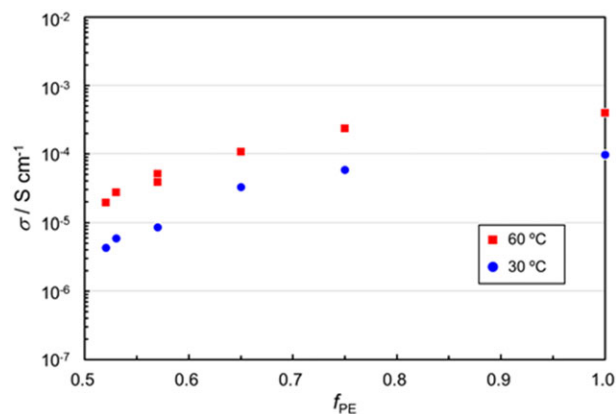


FIGURE 4 f_{PE} dependence of the conductivity for PSE_x s, $L-PSE_{0.73}$, and $PE_{0.85}$ at 30°C and 60°C . The data for $PSE_{1.00}$ at 30°C are removed due to its partially crystalline nature [Colour figure can be viewed at wileyonlinelibrary.com]

block in the block copolymers. Here, the influence of x on the ionic conductivity should be considered. As aforementioned that, according to a previous report, P-(EO-*r*-MEEGE) showed the maximum conductivity at $x = 0.8$ to 0.7 , and the conductivity at low x was about one-third of the maximum one.¹³ On comparing PSE_{0.41} and PSE_{0.75} with nearly the same f_{PE} (0.52-0.53), the ionic conductivities at 30°C were 4.36×10^{-6} and 5.92×10^{-6} S cm⁻¹, respectively, which are almost similar values, indicating that f_{PE} primarily determines the ionic conductivity. However, if we assume a simple distinct two-phase model with continuous PE segment phase, the conductivity should decrease in proportion to f_{PE} . The experimental results appear to reflect such assumption when $f_{PE} > 0.75$, where the PE continuous phase may be formed. On the contrary, the conductivity of PSE_{*x*}s having lower f_{PE} drastically decreased, where such simple assumptions cannot be applied and PSt domains greatly block the ion transport. According to the previously reported studies,^{24,26} a continuous phase of the block copolymer with small f_{PE} is hardly developed such as lamellae, whereas the continuous phase develops such as hexagonally perforated lamellae and hexagonally packed cylinders as the f_{PE} value increases. In our case, change in microphase separation structure may occur around $f_{PE} = 0.65$ to 0.75 .

Finally, we checked the ionic conductivity of L-PSE_{0.73} at high temperatures. Figure 5 shows Arrhenius plot of the ionic conductivity measured from 100°C to 0°C. The dashed line indicates the calculated value by using the Vogel-Tamman-Fulcher (VTF) parameters of L-PSE_{0.73} in Table S1. The conductivity at 100°C shifted to a higher value from the fitting line. The PE ion conduction path structure would collapse at the high temperature due to glass transition of the PSt segment. However, the segmental mobility of the PE chain can increase owing to the relaxation of the PSt segment. Jannasch et al have reported similar results utilizing an SPE consisting of LiTFSI and polyethylene-*b*-P-(EO-*r*-PO)-*b*-polyethylene (propylene oxide (PO)), where polyethylene segments act as hard segments.¹⁸ The ionic conductivity of the SPE increases because of the greater mobility of the PE segment above the T_m of polyethylene (100°C). In other words, the ionic conductivity deeply correlates with the softening temperature.

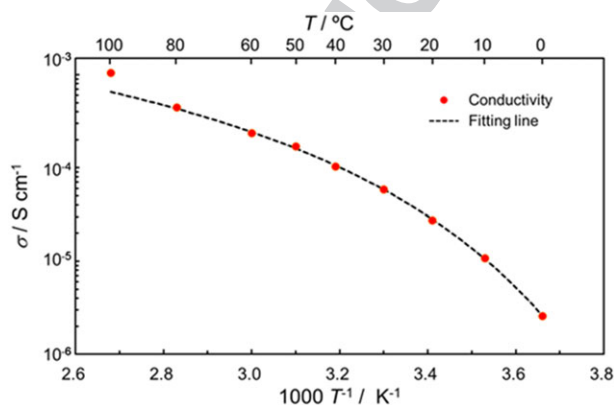


FIGURE 5 Temperature dependence of the ionic conductivity for Li-doped L-PSE_{0.73} with [Li]/[O] = 0.05 measured from 100°C to 0°C. The dashed line was fitted by using Equation S1 and the fitting parameters listed in Table S1 for L-PSE_{0.73} [Colour figure can be viewed at wileyonlinelibrary.com]

4 | CONCLUSIONS

We have synthesized diblock copolymers (PSE_{*x*}s) comprising PSt and PE block segments, which have several weight fractions of the PE segment ($f_{PE} = 0.52$ - 0.75) and several molar ratios of EO and MEEGE (EO ratio: $x = 0.41$ - 1.00), via one-pot anionic polymerization. To activate the PSt polymer ends, *t*-BuP₄ was used for ring-opening anionic polymerization reaction due to acceleration of the dissociation of the alcoholate-lithium ion pair ($-O^-Li^+$). A decrease in x (an increase in the MEEGE fraction) in the PE segment suppressed the crystallization of PEO segments. By introducing the MEEGE moiety, the PSE_{*x*}s showed high ionic conductivity owing to the suppression of the crystallization of PEO and fast molecular motion of the MEEGE side chains. The ionic conductivity was greatly affected by f_{PE} values, even though it was not simply in proportion to f_{PE} but appeared to be affected by block copolymer morphology.

ACKNOWLEDGEMENT

This work was partly supported by the Grants-in-Aid for Scientific Research S (15H05758) from the Ministry of Education, Culture, Sports, Science and Technology (MEXT) of Japan.

ORCID

Hisashi Kokubo  <https://orcid.org/0000-0001-9994-2863>

REFERENCES

- Armand MB, Chabango JM, Duclot MJ. *Fast ion transport in solids*. New York: North-Holland; 1979:131.
- Armand M. Polymer solid electrolytes—an overview. *Solid State Ion*. 1983;9-10:745-754.
- Watanabe M, Nagano S, Sanui K, Ogata N. Ionic conductivity of network polymers from poly-(ethylene oxide) containing lithium perchlorate. *Polym J*. 1986;18(11):809-817.
- Watanabe M, Ogata N. Ionic conductivity of polymer electrolytes and future applications. *Br Polym J*. 1988;20(3):181-192.
- Vallée A, Besner S, Prud'homme J. Comparative study of poly-(ethylene oxide) electrolytes made with LiN-(CF₃SO₂)₂, LiCF₃SO₃ and LiClO₄: thermal properties and conductivity behavior. *Electrochim Acta*. 1992;37:1579-1583-9.
- Sylla S, Sanchez JY, Armand M. Electrochemical study of linear and crosslinked POE-based polymer electrolytes. *Electrochim Acta*. 1992;37(9):1699-1701.
- Alloin F, Sanchez JY, Armand M. Electrochemical behavior of lithium electrolytes based on new polyether networks. *J Electrochem Soc*. 1994;141(7):1915-1920.
- Lascaud S, Perrier M, Vallée A, Besner S, Prud'homme J, Armand M. Phase diagrams and conductivity behavior of poly-(ethylene oxide)-molten salt rubbery electrolytes. *Macromolecules*. 1994;27(25):7469-7477.
- Gorecki W, Jeannin M, Belorizky E, Roux C, Armand M. Physical properties of solid polymer electrolyte PEO-(LiTFSI) complexes. *J Phys Condens Matter*. 1995;7(34):6823-6832.
- Motogami K, Kono M, Mori S, Watanabe M, Ogata N. A new polymer electrolyte based on polyglycidylether. *Electrochim Acta*. 1992;37(9):1725-1727.
- Watanabe M, Nishimoto A. Effects of network structures and incorporated salt species on electrochemical properties of polyether-based polymer electrolytes. *Solid State Ion*. 1995;79:306-312.

12. Nishimoto A, Watanabe M, Ikeda Y, Kohjiya S. High ionic conductivity of new polymer electrolytes based on high molecular weight polyether comb polymers. *Electrochim Acta*. 1998;43(10-11):1177-1184.
13. Watanabe M, Endo T, Nishimoto A, Miura K, Yanagida M. High ionic conductivity and electrode interface properties of polymer electrolytes based on high molecular weight branched polyether. *J Power Sources*. 1999;81-82:786-789.
14. Nishimoto A, Agehara K, Fruya N, Watanabe T, Watanabe M. High ionic conductivity of polyether-based network polymer electrolytes with hyperbranched side chains. *Macromolecules*. 1999;32(5):1541-1548.
15. Watanabe M, Hirakimoto T, Mutoh S, Nishimoto A. Polymer electrolytes derived from dendritic polyether macromonomers. *Solid State Ion*. 2002;148(3-4):399-404.
16. Gorecki W, Roux C, Clémancey M, Armand M, Belorizky E. NMR and conductivity study of polymer electrolytes in the imide family: P(EO)/Li₊ [N(SO₂C_nF_{2n+1})(SO₂C_mF_{2m+1})]. *Chemphyschem*. 2002;3(7):620-625.
17. Zhang H, Liu C, Zheng L, et al. Lithium bis-(fluorosulfonyl)imide/poly(ethylene oxide) polymer electrolyte. *Electrochim Acta*. 2014;133:529-538.
18. Jannasch P. Ionic conductivity in physical networks of polyethylene-polyether-polyethylene triblock copolymers. *Chem Mater*. 2002;14(6):2718-2724.
19. Metwalli E, Nie M, Körstgens V, Perlich J, Roth SV, Müller-Buschbaum P. Morphology of lithium-containing diblock copolymer thin films. *Macromol Chem Phys*. 2011;212(16):1742-1750.
20. Singh M, Odusanya O, Wilmes GM, et al. Effect of molecular weight on the mechanical and electrical properties of block copolymer electrolytes. *Macromolecules*. 2007;40(13):4578-4585.
21. Panday A, Mullin S, Gomez ED, et al. Effect of molecular weight and salt concentration on conductivity of block copolymer electrolytes. *Macromolecules*. 2009;42(13):4632-4637.
22. Wanakule NS, Panday A, Mullin SA, Gann E, Hexemer A, Balsara NP. Ionic conductivity of block copolymer electrolytes in the vicinity of order-disorder and order-order transitions. *Macromolecules*. 2009;42(15):5642-5651.
23. Mullin SA, Stone GM, Panday A, Balsara NP. Salt diffusion coefficients in block copolymer electrolytes. *J Electrochem Soc*. 2011;158(6):A619-A627.
24. Young WS, Epps TH. Ionic conductivities of block copolymer electrolytes with various conducting pathways: sample preparation and processing considerations. *Macromolecules*. 2012;45(11):4689-4697.
25. Stone GM, Mullin SA, Teran AA, et al. Resolution of the modulus versus adhesion dilemma in solid polymer electrolytes for rechargeable lithium metal batteries. *J Electrochem Soc*. 2012;159(3):A222-A227.
26. Yuan R, Teran AA, Gurevitch I, Mullin SA, Wanakule NS, Balsara NP. Ionic conductivity of low molecular weight block copolymer electrolytes. *Macromolecules*. 2013;46(3):914-921.
27. Chintapalli M, Chen XC, Thelen JL, et al. Effect of grain size on the ionic conductivity of a block copolymer electrolyte. *Macromolecules*. 2014;47(15):5424-5431.
28. Young NP, Devaux D, Khurana R, Coates GW, Balsara NP. Investigating polypropylene-poly(ethylene oxide)-polypropylene triblock copolymers as solid polymer electrolytes for lithium batteries. *Solid State Ion*. 2014;263:87-94.
29. Schulze MW, McIntosh LD, Hillmyer MA, Lodge TP. High-modulus, high-conductivity nanostructured polymer electrolyte membranes via polymerization-induced phase separation. *Nano Lett*. 2014;14(1):122-126.
30. Devaux D, Gle D, Phan TNT, et al. Optimization of block copolymer electrolytes for lithium metal batteries. *Chem Mater*. 2015;27(13):4682-4692.
31. Zardalidis G, Pipertzis A, Mountrichas G, Pispas S, Mezger M, Floudas G. Effect of polymer architecture on the ionic conductivity. Densely grafted poly-(ethylene oxide) brushes doped with LiTf. *Macromolecules*. 2016;49(7):2679-2687.
32. Sarapas JM, Saijo K, Zhao Y, Takenaka M, Tew GN. Phase behavior and H⁺ ion conductivity of styrene-ethylene oxide multiblock copolymer electrolytes. *Polym Adv Technol*. 2016;27(7):946-954.
33. Jo G, Kim O, Kim H, Choi UH, Lee SB, Park MJ. End-functionalized block copolymer electrolytes: effect of segregation strength on ion transport efficiency. *Polym J*. 2016;48(4):465-472.
34. Lassagne A, Beaudoin E, Ferrand A, et al. New approach to design solid block copolymer electrolytes for 40°C lithium metal battery operation. *Electrochim Acta*. 2017;238:21-29.
35. Metwalli E, Kaeppl MV, Schaper SJ, et al. Conductivity and morphology correlations of ionic-liquid/lithium-salt/block copolymer nanostructured hybrid electrolytes. *ACS Appl Energy Mater*. 2018;1(2):666-675.
36. Xu H, Wang A, Liu X, et al. A new fluorine-containing star-branched polymer as electrolyte for all-solid-state lithium-ion batteries. *Polymer*. 2018;146:249-255.
37. Khandpur AK, Förster S, Bates FS, et al. Polyisoprene-polystyrene diblock copolymer phase diagram near the order-disorder transition. *Macromolecules*. 1995;28(26):8796-8806.
38. Tsuda R, Kodama K, Ueki T, Kokubo H, Imabayashi S, Watanabe M. LCST-type liquid-liquid phase separation behaviour of poly-(ethylene oxide) derivatives in an ionic liquid. *Chem Commun*. 2008; (40):4939-4941.
39. Kodama K, Tsuda R, Niitsuma K, et al. Structural effects of polyethers and ionic liquids in their binary mixtures on lower critical solution temperature liquid-liquid phase separation. *Polym J*. 2011;43(3):242-248.
40. Quirk RP, Kim J, Kausch C, Chun M. Butyllithium-initiated anionic synthesis of well-defined poly-(styrene-block-ethylene oxide) block copolymers with potassium salt additives. *Polym Int*. 1996;39(1):3-10.
41. Esswein B, Möller M. Polymerization of ethylene oxide with alkyllithium compounds and the phosphazene base "tBu-P₄". *Angew Chem Int Ed*. 1996;35(6):623-625.
42. Förster S, Krämer E. Synthesis of PB-PEO and PI-PEO block copolymers with alkyllithium initiators and the phosphazene base t-BuP₄. *Macromolecules*. 1999;32(8):2783-2785.
43. Toy AA, Reinicke S, Müller AHE, Schmalz H. One-pot synthesis of polyglycidol-containing block copolymers with alkyllithium initiators using the phosphazene base t-BuP₄. *Macromolecules*. 2007;40(15):5241-5244.
44. Santangelo PG, Roland CM. Molecular weight dependence of fragility in polystyrene. *Macromolecules*. 1998;31(14):4581-4585.

SUPPORTING INFORMATION

Additional supporting information may be found online in the Supporting Information section at the end of the article.

How to cite this article: Kokubo H, Nakazawa E, Watanabe M. Solid polymer electrolytes based on polystyrene-polyether block copolymers having branched ether structure. *Polym Adv Technol*. 2018;1-7. <https://doi.org/10.1002/pat.4511>